ONLINE SUPPLEMENTARY INFORMATION

Identification of a novel Wnt5a-CK1ε-Dvl2-Plk1-mediated primary cilia disassembly pathway

Kyung Ho Lee, Yoshikazu Johmura, Li-Rong Yu, Jung-Eun Park, Yuan Gao, Jeong K. Bang, Ming Zhou, Timothy D. Veenstra, Bo Yeon Kim, and Kyung S. Lee

Supplementary Materials and methods

Plasmid constructions

A *Bam*HI-*Eco*RI fragment from mouse Dvl2 wild-type (WT) or various mutants was subcloned into pcDNA-FLAG (Invitrogen, Carlsbad, CA), pGEX-4T-2 (Amersham Biosciences, Piscataway, NJ), or pHR′-CMV-SV-puro (a gift of Chou-Zen Giam, Uniformed Services University of the Health Sciences, Bethesda, MD) digested with the corresponding enzymes. The *Bam*HI-*Eco*RI fragment was generated by polymerase chain reaction (PCR) using pCS2+-Flag-mouse Dvl2 (a gift of Sean B. Lee, National Institutes of Health, Bethesda, MD) as a template. Mutants were generated by PCR-based site-directed mutagenesis. *Sma*I-*Not*I fragments of CK1δ WT, CK1ε WT, and the corresponding kinase-inactive CK1ε (K38A) mutant were amplified by PCR from the respective pCS2+-Myc6-CK1δ WT, pCS2+-CK1ε WT, and pCS2+-CK1ε (K38A) constructs (gifts of Dave Virshup, Institute of Medical Biology, Singapore), and subcloned into pGEX-4T-2 (Amersham Biosciences). *EcoR*I-*Not*I fragments of HEF1 WT were amplified by PCR from pCMV-Flag-HEF1 WT (a gift of Joel Raingeaud,

INSERM, France), and subcloned into pGEX-4T-2 (Amersham Biosciences). All the PCR products were confirmed by sequencing analysis. To express hemagglutinin (HA)-Plk1 under Cytomegalovirus (CMV) promoter control, the pHR′-CMV-SV-puro vector digested with *Sal*I (end-filled) was ligated with an end-filled *Sal*I-*Not*I fragment of HA-tagged mouse Plk1 WT or the corresponding kinase-inactive K82M mutant excised from the respective pCI-neo-HA-Plk1 constructs.

To generate lentivirus-based Dvl2 shRNA constructs, the oligonucleotide sequences corresponding to nt 776-794 of human Dvl2 (forward 5′-CCGGCCACAATGTCTCTCAATATGCTAGCATATTGAGAGACATTGTGGTTTTTG-3′ and reverse 5′-AATTCAAAAACCACAATGTCTCTCAATATGCTAGCATATTGAGAGACATTGTGG-3′; targeting sequences are underlined) were annealed and inserted into pLKO.1-puro vector (a gift from S.A. Stewart and P.A. Sharp, Massachusetts Institute of Technology, Cambridge, MA) digested with *Age*I and *EcoR*I. All the Dvl2 constructs expressed in hTERT-RPE or HeLa cells are derived from the mouse Dvl2 gene. Dvl2 mutant alleles bearing silent mutation(s) against sh776 were generated by PCR-based mutagenesis. The sh776-insensitive silent mutant allele contains 5′-CAACTATGTCCCTAAA**C**AT-3′ (from nt 776 to 794 in human Dvl2) that bears four silent mutations (underlined) and one non-conserved base (boldface C) between mouse and human clones. All the lentivirus-based shRNA and synthetic siRNA target sequences are provided in Table S1.

Virus generation and infection

For the production of shRNA lentiviruses, pLKO.1-puro-shLuciferase (shLuc), -shDvl2, -shPlk1, -shAurA, -shβ-catenin, -shCK1δ, -shCK1ε or –shHEF1 was co-transfected with pHR′-CMVΔR8.2Δvpr and pHR′-CMV-VSV-G (protein G of vesicular stomatitis virus) into 293T cells. To generate lentiviruses expressing wild-type Dvl2, Dvl2 (S143A), Dvl2 (T224A), Dvl2 (S143A/T224A), HA-mPlk1 WT, HA-mPlk1 (K82M), Flag-HEF1 WT or Flag-HEF1 (7A), corresponding pHR′- CMV-SV-puro-based constructs were co-transfected with pHR′-CMVΔR8.2Δvpr and pHR′-CMV-VSV-G. Stable HeLa or hTERT-RPE cell lines expressing various Dvl2 or Plk1 constructs were generated by infecting the cells with respective lentiviruses and selecting them with puromycin (4 μg/ml for HeLa and 20 μg/ml for hTERT-RPE) for 2–3 days. Adenoviruses expressing either wild-type Plk1 or kinase-inactive Plk1 (K82M) have been described previously (Seong *et al*, 2002).

Cell culture, synchronization, inhibitor treatment, transfection, and flow cytometry analysis

Cell lines were cultured as recommended by American Type Culture Collection (Manassas, VA). hTERT-RPE *Plk1-as* cells (Burkard *et al*, 2007) were obtained as a gift of Prasad Jallepalli (Memorial Sloan-Kettering Cancer Center, New York, NY). To arrest cells in S or M phase, cells were treated with 2.5 mM of thymidine (Sigma, St. Louis, MO) or 200 ng/ml of nocodazole (Sigma) for 18 h. To generate quiescent G0 cells, cells were serum-starved for 48 h. Where indicated, cells were then treated with serum to induce cell cycle entry. Control or Wnt5a-containing conditional medium (CM) was prepared from L cells or L cells expressing Wnt5a (a gift of Sean B. Lee).

To inhibit CK1δ/ε, GSK3β, AurA, Plk1, or Cdc2, HeLa, and hTERT-RPE cells were treated with 40 μM of IC261 (Calbiochem, San Diego, CA) {a concentration similar to that used in previous reports (Tillement *et al*, 2008; Gao *et al*, 2002)}, 100 nM of GSK Inhibitor X (Calbiochem), 600 nM of VX-680 (ChemieTek, Indianapolis, IN), 100 nM of BI 2536 (ChemieTek) or 150 nM of GSK461364A (a gift of GlaxoSmithKline, Research Triangle Park, NC), or 200 nM of BMI-1026 (Seong *et al*, 2003), respectively. Treatment of cells with all the inhibitors was carried out for 3 h, except BMI-1026, which was for 30 min.

Plasmid transfection was carried out using Lipofectamine 2000 (Invitrogen). For siRNA transfection, cells were transfected with 100 nM of siRNA using Oligofectamine (Invitrogen), according to manufacturer's instructions.

For flow cytometry (FACS) analysis, cells seeded into a 6-well culture dish were harvested by trypsinization, fixed with ethanol, and then stained with propidium iodide (Sigma) at the final concentration of 1mg/ml. FACS analyses were carried out using FACScan (Becton Dickinson, San Jose, CA) and data were analyzed by the Flowjo program (Tree Star, San Carlos, CA).

Immunoprecipitation, λ-phosphatase treatment, antibody production, and immunoblotting

Immunoprecipitation was carried out essentially as described previously (Lee *et al*, 1995) in TBSN buffer {20 mM Tris-Cl (pH8.0), 150 mM NaCl, 0.5% NP-40, 5 mM EGTA, 1.5 mM EDTA, 0.5 mM Na_3VO_4**,** and 20 mM *p*-nitrophenyl phosphate}. Briefly, cleared cell lysates were incubated with indicated antibodies for 4 h at 4°C and then added with

protein A or G–sepharose beads (Santa Cruz Biotechnologies, Santa Cruz, CA) for an additional 2 h incubation. Immunoprecipitated proteins were separated by sodium dodecyl sulfate-polyacrylamide gel electrophoresis (SDS-PAGE) and transferred to the PVDF membrane. Where indicated, samples were separated by low-bis (96:1 acrylamide:bis-acrylamide mixture) SDS–PAGE or 50 μM, Mn^{2+} Phos-tag gels to separate proteins according to the level of phosphorylation. Membranes were sequentially incubated with indicated primary and horseradish peroxidase (HRP)-conjugated secondary antibodies (Amersham Biosciences). Immunoreactive signals were detected by enhanced chemiluminescence (ECL) detection system (Pierce, Rockford, IL). Relative signal intensities from immunoblots were determined by quantifying the individual signals with Image J software.

Where indicated, immunoprecipitates were sequentially washed with phosphatase inhibitor-absent TBSN and 1X phosphatase buffer {50 mM Tris-Cl (pH7.5), 100 mM NaCl, 0.1 mM EGTA, 2 mM DTT, and 2 mM $MnCl_2$}, and then reacted with λ phosphatase in 1X phosphatase buffer for 30 min at 30°C.

In vitro kinase assays

For the *in vitro* kinase assay, GST-Dvl2, GST-HEF1, GST-CK1δ WT, and GST-CK1ε WT and the corresponding CK1ε (K38A) mutant were purified from *E. coli* BL21 (DE3) with glutathione (GSH)-agarose (Sigma). Both wild-type and kinase-inactive HA-Plk1 (K82M) (Lee *et al*, 1995) were purified from Sf9 cells. In vitro kinase reactions were carried out in a kinase cocktail {50 mM Tris-Cl (pH 7.5), 10 mM $MgCl_2$, 5 mM dithiothreitol, 2 mM EGTA, 0.5 mM Na_3VO_4, and 20 mM *p*-nitrophenyl phosphate} in

the presence of 100 μM ATP (10 μCi of [γ-^{32}P]ATP) for 30 min at 30°C. Reactions were terminated by the addition of 2X SDS sample buffer. Boiled samples were subjected to SDS-PAGE, stained with Coomassie, dried, and then subjected to an autoradiogram.

For immunoprecipitation kinase assays, anti-CK1ε immunoprecipitates were reacted in the presence of 10 μM cold ATP and 10 μCi of [γ-^{32}P]ATP at 30°C for 30 min. A set of resulting samples was separated by SDS-PAGE and exposed (Autorad), while another set of the samples was subjected to immunoblotting analyses to determine the amount of CK1ε immunoprecipitated for each lane.

In vivo ubiquitinylation assay

HeLa cells were transfected with either HA-ubiquitin (Ub) or together with Flag-β-catenin construct (a gift from Eric R. Fearon, Univ. of Michigan, Ann Arbor, MI). Where indicated, cells were infected with adenoviruses expressing either EGFP-Plk1 WT or the corresponding kinase-inactive K82M mutant 4 h after transfection. The cells were then treated with nocodazole for 18 h before harvest. To acutely inhibit Plk1 activity, cells were treated with 100 nM of BI 2536 or 150 nM of GSK461364A for 3 h before harvest. To prevent proteasomal degradation of β-catenin, cells were also treated with 10 μM of MG132 for 3 h prior to harvest. Forty-two hours after transfection, cells were harvested for immunoprecipitation as described above.

Luciferase reporter assay and ELISA-based Plk1 kinase assay

To monitor the β-catenin-dependent signaling event, we used TCF reporter system, SuperTopFlash (TCF reporter plasmid) and the respective negative control FopFlash

(TCF binding site mutant). To carry out luciferase assays, HeLa cells were transfected with SuperTopFlash and FopFlash reporter plasmids (gifts of Randall T. Moon, University of Washington, Seattle, WA). pRL-TK expressing Renilla luciferase (Promega, Madison, WI) was co-transfected as a control for transfection efficiency. The resulting cells were then treated with either control or Wnt3a-containing CM. Luciferase assays were performed with a Dual luciferase assay kit (Promega) and luciferase activities were quantified by Veritas microplate luminometer (Turner Biosystems, Sunnyvale, CA). Firefly luciferase values were normalized by Renilla luciferase activities from the same sample.

To quantify Plk1 kinase activity, total cellular lysates were prepared from hTERT-RPE or hTERT-RPE *Plk1-as* cells, and then ELISA-based kinase assays were carried out as described previously (Park *et al*, 2009).

Semi-quantitative RT-PCR

Total RNA was extracted from hTERT-RPE cells expressing various Dvl2 constructs using TRIzol Reagent (Invitrogen). cDNA was generated by SuperScript III Reverse Transcriptase (Invitrogen) according to the manufacturer's instructions. For semi-quantitative RT-PCR, PCR cycles were adjusted to ensure that PCR products were obtained from within the exponential phase of DNA amplification. PCR was performed using a DNA Thermal Cycler (MJ Research, Waltham, MA) with the conditions of 94°C for 1 min, 55°C for 1 min, and 72°C for 1 min for a total of 28 cycles for HEF1 or 22 cycles for β-actin, followed by a 5-min extension at 72°C. PCR products were electrophoresed in 1% agarose gel, stained with ethidium bromide, and photo-scanned.

Resulting DNA bands were quantified using Image J software. For HEF1 amplification, forward, 5′-TCACCACAACCATCAACACC-3′ and reverse, 5′-GCAGTCCCCTTCCTCTTTTT-3′ primers were used. For β-actin amplification, forward, 5′-TGGCACCACACCTTCTACAATGAGC-3′ and reverse, 5′-TGTCACGCACGATTTCCCTCTCAG-3′ primers were used.

Mass spectrometry analysis

HeLa cells were transfected with pFlag-Dvl2 or pFlag-HEF1 and treated with 2.5 mM thymidine (Sigma) or 200 ng/ml of nocodazole (Sigma) for 18 h to arrest the cells in S or M phase. Flag-Dvl2 or Flag-HEF1 was immunoprecipitated with anti-FLAG M2 Affinity Gel (Sigma), separated by 10% SDS-PAGE, and stained with GelCode Blue Stain Reagent (Pierce). The Flag-Dvl2 or Flag-HEF1 band was excised from the gel and then in-gel digested with trypsin (Promega) for mass spectrometry analysis as described previously (Soung *et al*, 2009). Briefly, the peptides from in-gel digested Flag-Dvl2 or Flag-HEF1 were separated using nanoflow reversed-phase liquid chromatography, which was coupled online to an LTQ linear ion trap or LTQ-Orbitrap XL mass spectrometer (Thermo Electron, San Jose, CA) for MS/MS and MS/MS/MS analysis (nanoLC-MS^2-MS^3). Peptide separation was performed at a flow rate of ~250 nL/min using a step gradient of 2%–42% solvent B (0.1% formic acid in acetonitrile) for 40 min, 42%–98% solvent B for 10 min and 98%–98% solvent B for 5 min, while mobile phase A was 0.1% formic acid in water. The mass spectrometer was operated in a data-dependent mode to sequentially acquire MS, MS^2, and neutral phosphate loss-dependent MS^3 spectra with dynamic exclusion. Normalized collision energy was 35% for both MS^2 and MS^3. The

raw MS^2 and MS^3 data were searched using SEQUEST (Thermo Electron) against a protein database including Flag-Dvl2 or Flag-HEF1 to identify phosphopeptides. The identified tryptic phosphopeptides were further subjected to manual validation of the peptide sequence and phosphorylation sites by examining the corresponding MS^2 and/or MS^3 spectra.

GST-PBD binding, peptide-binding, and peptide competition assays

To carry out Plk1 PBD pull-down assays, bead-associated GST-PBD WT or GST-PBD (AM) mutant was incubated with total cellular lysates prepared in TBSN or RIPA {50 mM Tris-Cl (pH7.4), 150 mM NaCl, 1% NP40, 0.5% Na-deoxycholate, 0.1% SDS, 1X protease inhibitor cocktail, and 20 mM *p*-nitrophenyl phosphate} buffer for 2 h, and then precipitated. The precipitates were washed with TBSN buffer 4 times before analyses. For accurate comparison of the amount of proteins in each sample, precipitates were treated with λ-phosphatase, where indicated, to reduce all the phospho-dependent slow-migrating forms to non-phosphorylated form. Samples were then subjected to immunoblotting analyses.

Dvl2 peptides conjugated with an N-terminal NH_2-C-$(CH2)_6$ linker were cross-linked to the beads using SulfoLink Coupling gel (Pierce). The obtained immobilized peptides were incubated with HeLa cell lysates for 2 h at 4°C and washed with TBSN buffer 4 times. The resulting samples were analyzed by immunoblotting analyses.

To perform peptide competition assays, HeLa cell lysates prepared in TBSN were incubated with 0.4 mM of the indicated peptide for 15 min at 4°C, and then subjected to GST-PBD pull-downs.

Immunofluorescence analyses

To detect centrosomally localized Dvl2, Dvl2 p-S143 and p-T224 epitopes, CK1δ, and CK1ε, hTERT-RPE cells were extracted with extraction buffer {0.5% Triton X-100 in 80 mM PIPES (pH 6.8), 1 mM $MgCl_2$, and 1 mM EGTA} for 30 sec and fixed with −20°C methanol for 5 min. The samples were then washed with 1X PBS + 0.1% Triton X-100 (PBST) 4 times. Immunostaining was carried out as described previously (Seong *et al*, 2002) with Alexa Fluor 488 (green)- or Texas Red (red)-conjugated secondary antibodies (Invitrogen). To stain DNA, cells were treated with PBS containing 0.1 μg/ml of 4′,6′-diamidino-2-phenylindole (DAPI) (Sigma). Digital images were collected with a Zeiss LSM510 confocal microscope. To quantify centrosomal fluorescence intensities, confocal images (1024x1024 pixels and 16-bit resolution) of unsaturated fluorescence signals were acquired at 0.4 μm intervals with the same laser intensity, and fluorescence intensities were determined from identifiable centrosomes using Zeiss AIM confocal software. The antibodies used were: rabbit anti-Dvl2 (Cell Signaling, 1:200), rabbit anti-Dvl2 p-S143 (this study, 1:100), rabbit anti-Dvl2 p-T224 (this study, 1:100), FITC-conjugated goat anti-γ-tubulin (Santa Cruz Biotechnologies, 1:20), mouse anti-CK1δ (Santa Cruz Biotechnologies, 1:50), and mouse anti-CK1ε (BD Transduction Lab., 1:100).

Analysis of primary cilia disassembly and neutralization of Wnt5a

hTERT-RPE cells were grown in DME/F-12 1:1 medium (Hyclone, Logan, UT) with 10% Tet System-approved fetal bovine serum (Clontech, Mountain View, CA). NIH 3T3 cells were cultured in DMEM (Invitrogen, Carlsbad, CA) plus 10% calf serum

(Invitrogen). To induce primary cilia, hTERT-RPE or NIH 3T3 cells were cultured under serum starvation for 48 h. To analyze primary cilia disassembly, less than 30% cells were seeded and cultured on cover slips for 24 h. Following serum starvation for 48 h, the resulting cells were then provided with either fetal bovine serum (for hTERT-RPE) or calf serum (for NIH 3T3) at the final concentration of 10% to induce primary cilia disassembly. Cells were fixed at various time points after serum stimulation, immunostained with mouse anti-acetylated α-tubulin (Sigma), FITC-conjugated goat anti-γ-tubulin (Santa Cruz Biotechnologies), or rabbit anti-Cyclin A (Santa Cruz Biotechnologies) antibodies. To measure the length of primary cilia, images were acquired by Zeiss LSM 510 confocal microscope at 1024 X 1024 pixels and 12-bit resolution, and analyzed by Zeiss AIM software.

To neutralize Wnt5a activity, control or Wnt5a-containing CM was preincubated with control goat IgG or goat anti-Wnt5a antibody (R&D systems, Minneapolis, MN) at the final concentration of 5 μg/ml at 4°C for 24 h and then used.

Supplementary References

Burkard ME, Randall CL, Larochelle S, Zhang C, Shokat KM, Fisher RP, Jallepalli PV (2007) Chemical genetics reveals the requirement for Polo-like kinase 1 activity in positioning RhoA and triggering cytokinesis in human cells. *Proc Natl Acad Sci, U S A* **104:** 4383-4388

Dadke D, Jarnik M, Pugacheva EN, Singh MK, Golemis EA (2006) Deregulation of HEF1 impairs M-phase progression by disrupting the RhoA activation cycle. *Mol Biol Cell* **17:** 1204-1217

Elbashir SM, Harborth J, Lendeckel W, Yalcin A, Weber K, Tuschl T (2001) Duplexes of 21-nucleotide RNAs mediate RNA interference in cultured mammalian cells. *Nature* **411:** 494-498

Gilmartin AG, Bleam MR, Richter MC, Erskine SG, Kruger RG, Madden L, Hassler DF, Smith GK, Gontarek RR, Courtney MP*, et al* (2009) Distinct concentration-dependent effects of the polo-like kinase 1-specific inhibitor GSK461364A, including differential effect on apoptosis. *Cancer Res* **69:** 6969-6977

Hansen DV, Loktev AV, Ban KH, Jackson PK (2004) Plk1 regulates activation of the anaphase promoting complex by phosphorylating and triggering SCFbetaTrCP-dependent destruction of the APC Inhibitor Emi1. *Mol Biol Cell* **15:** 5623-5634

Lee KS, Yuan Y-L, Kuriyama R, Erikson RL (1995) Plk is an M-phase-specific protein kinase and interacts with a kinesin-like protein, CHO1/MKLP-1. *Mol Cell Biol* **15:** 7143-7151

Lenart P, Petronczki M, Steegmaier M, Di Fiore B, Lipp JJ, Hoffmann M, Rettig WJ, Kraut N, Peters JM (2007) The small-molecule inhibitor BI 2536 reveals novel insights into mitotic roles of polo-like kinase 1. *Curr Biol* **17:** 304-315

Park J-E, Li L, Park J, Knecht R, Strebhardt K, Yuspa SH, Lee KS (2009) Direct quantification of polo-like kinase 1 activity in cells and tissues using a highly sensitive and specific ELISA assay. *Proc Natl Acad Sci USA* **106:** 1725-1730

Perez-Ruiz A, Ono Y, Gnocchi VF, Zammit PS (2008) beta-Catenin promotes self-renewal of skeletal-muscle satellite cells. *J Cell Sci* **121:** 1373-1382

Pugacheva EN, Jablonski SA, Hartman TR, Henske EP, Golemis EA (2007) HEF1-dependent Aurora A activation induces disassembly of the primary cilium. *Cell* **129:** 1351-1363

Schwarz-Romond T, Metcalfe C, Bienz M (2007) Dynamic recruitment of axin by Dishevelled protein assemblies. *J Cell Sci.* **120:**2402-2412

Seong YS, Kamijo K, Lee JS, Fernandez E, Kuriyama R, Miki T, Lee KS (2002) A spindle checkpoint arrest and a cytokinesis failure by the dominant-negative polo-box domain of Plk1 in U-2 OS cells. *J Biol Chem* **277:** 32282-32293

Seong YS, Min C, Li L, Yang JY, Kim SY, Cao X, Kim K, Yuspa SH, Chung HH, Lee KS (2003) Characterization of a novel cyclin-dependent kinase 1 inhibitor, BMI-1026. *Cancer Res* **63:** 7384-7391

Soung NK, Park JE, Yu LR, Lee KH, Lee JM, Bang JK, Veenstra TD, Rhee K, Lee KS (2009) Plk1-dependent and -independent roles of an ODF2 splice variant, hCenexin1, at the centrosome of somatic cells. *Dev Cell* **16:** 539-550

Supplementary Figure Legends

Figure S1. Cell cycle-dependent regulation of Dvl2. To monitor the expression level of Dvl2 during the cell cycle, HeLa cells were arrested at the G1/S boundary (G1/S) by double thymidine block, and then released into nocodazole (Noc)-containing medium. Total lysates prepared from cells harvested at the indicated time points after release were either untreated or treated with λ phosphatase (λ PPase), and then analyzed by immunoblotting analyses. Note that dephosphorylation of Dvl2 in the total lysates by λ phosphatase treatment was not as efficient as that of Dvl2 in GST-PBD precipitates in Figures 2B and 6A. The levels of dephosphorylated Cdc25C and Axin1 in the λ phosphatase-treated samples serve as controls for dephosphorylated proteins.

Figure S2. Identification of conserved S143 and T224 residues as CK1δ/ε-dependent phosphorylation sites on Dvl2. (A) HeLa cells transfected with Flag-Dvl2 were treated with thymidine for 18 h and harvested. The resulting cells were subjected to immunoprecipitation analyses with control IgG or anti-Flag antibody. After separating the immunoprecipitates by SDS-PAGE, Flag-Dvl2 was excised from the gel and analyzed by mass spectrometry. **(B)** MS/MS spectra of the phosphopeptides containing S143 (upper) and T224 (lower), respectively. The phosphorylation sites were determined by the phosphorylated (red) fragment ions with (w/) or without (w/o) neutral loss of phosphate and unphosphorylated (blue) fragment ions. Major fragment ions are annotated in the MS/MS spectra. **(C, D)** Sequence alignment among the Dvl2 homologs from the indicated species (**C**) and the Dv11–3 isoforms from human (**D**). The S143 and T224 residues are marked in red. **(E)** *In vitro* kinase assays were carried out with bacterially

purified GST-CK1δ and GST-CK1ε, and phosphorylation sites on GST-Dvl2 were determined by mass spectrometry analyses. Identified phosphopeptides from the analyses and the frequency of peptide retrieval from each reaction are shown.

Figure S3. Plk1 does not function in the Wnt canonical pathway. (A) To examine whether Plk1 contributes to the regulation of β-catenin stability, HeLa cells were transfected with HA-Ub and infected with adenoviruses expressing either wild-type Plk1 (WT) or the corresponding kinase-inactive K82M mutant (KM) (Lee *et al*, 1995). To prevent protein degradation, the cells were treated with 10 μM MG132 for 3 h prior to harvest. Endogenous β-catenin was immunoprecipitated from soluble lysates and then immunoblotted with anti-HA antibody to detect HA-Ub-conjugated to β-catenin. The same membrane was stained with Coomassie (CBB) for loading controls. **(B)** HeLa cells were transfected with Flag-β-catenin and HA-Ub, and arrested with nocodazole to trap the cells in mitosis. Three hours prior to harvest, the cells were treated with MG132 and either control DMSO or one of the previously characterized Plk1 inhibitors (BI 2536 or GSK461364A) (Gilmartin *et al*, 2009; Lenart *et al*, 2007). The resulting cells were harvested and subjected to anti-Flag immunoprecipitation followed by anti-HA immunoblotting analysis. DM, DMSO; BI, BI 2536; GSK, GSK461364A. The disappearance of hyperphosphorylated Cdc25C indicates that both BI 2536 and GSK461364 effectively inhibited Plk1 activity. Note that the level of ubiquitinylated β-catenin was unaltered under these conditions. **(C)** HeLa cells were first infected with lentivirus expressing either control shLuciferase (shGL) or shPlk1, and then selected. To measure the β-catenin-dependent transcriptional activity, the cells were transfected with

the indicated Firefly luciferase reporter (TopFlash or FopFlash) and control Renilla luciferase, and then treated with thymidine/nocodazole and Wnt3a as shown in the schedule **(right)**. A luciferase assay was carried out as described in the Materials and Methods. Error bars, standard deviation.

Figure S4. Dvl2 is a negative regulator for primary cilia generation in both hTERT-RPE and NIH 3T3 cells. (A, B) Depletion of Dvl2 enhances ciliogenesis in hTERT-RPE cells. Cells were infected with lentivirus encoding either control shLuciferase (shGL) or one of the shRNA sequences targeting Dvl2 (sh35 or sh776), and then treated with puromycin one day after infection. Three days after puromycin selection, a set of samples was immunoblotted with anti-Dvl2 antibody and the resulting membrane was stained with Coomassie (CBB) **(A)**. Numbers for the RNAi sequences indicate the starting nucleotide positions of each shRNA in human Dvl2 nucleotide sequence (Genbank Accession number: BT009822). **(B)** Another set of samples from **(A)** was serum-starved for 48 h, fixed, and immunostained to quantify the fraction of cells with primary cilia. Greater than 300 cells were counted from each sample. Error bars, standard deviation. Note that the fraction of cells with primary cilia is inversely correlated with the level of Dvl2 present in the shGL-, sh35-, or sh776-treated cells in **(A)**. For efficient knockdown of Dvl2, sh776 lentivirus (denoted as shDvl2 hereafter) was used for all other experiments. The results shown here are consistent with the data in Figure 4A–D that demonstrate that Dvl2 is required for primary cilia disassembly. **(C–E)** Inhibition of primary cilia assembly by overexpression of Dvl2. hTERT-RPE cells overexpressing shRNA-insensitive Dvl2 (no tag) were infected with lentivirus expressing either control

shLuciferase (shGL) or shDvl2. The resulting cells were grown asynchronously and immunoblotted to determine the level of Dvl2 overexpression **(C)**. The cells in (**C**) were serum-starved for 48 h, fixed, immunostained (**D**), and then quantified (**E**). Magnified images for ciliated cells are shown at the bottom right corner in **(D)**. As reported previously (Schwarz-Romond *et al*, 2007), Dvl2 aggregates were frequently observed in Dvl2-overexpressed cells **(E, right)**. Remarkably, the depletion of endogenous Dvl2 negated the effect of overexpressed Dvl2 on primary cilia disassembly, even though the amount of overexpressed Dvl2 still far exceeds the normal level of endogenous Dvl2. Our results suggest that, although a role of aggregated Dvl2 assemblies has been suggested in the activation of β-catenin-dependent transcriptional regulation (Schwarz-Romond *et al*, 2007), only a fraction of overexpressed Dvl2 could be functional as a signaling molecule in the primary cilia disassembly pathway. **(F–H)** Depletion of Dvl2 delays primary cilia disassembly in NIH 3T3 cells. Cells were infected with lentivirus expressing either control shLuciferase (shGL) or sh776 (shDvl2). The resulting cells were harvested and immunoblotted to determine the level of Dvl2 depletion **(F)**. To examine the effect of Dvl2 depletion in primary cilia disassembly, the cells generated in (**F**) were serum-starved for 48 h and fixed at the indicated time points after serum stimulation. The resulting cells were immunostained (**G**) and quantified (**H**). Magnified images are shown at the bottom left corner. Greater than 300 cells were counted from each sample. Error bars, standard deviation. **(I)**, To compare the effect of siRNA, shRNA, or empty lentivirus itself on primary cilia formation, hTERT-RPE cells were either mock-treated, transfected with siLuciferase (siGL), or infected with lentivirus expressing shLuciferase (shGL) or empty vector itself. The resulting cells were serum-starved for 48 h, and then

immunostained with anti-acetylated tubulin and DAPI for quantification. Greater than 300 cells were counted for each sample. Bars, standard deviation. Note that cells infected with lentiviruses (shGL and empty lentivirus infected) formed primary cilia less efficiently than the cells transfected with siLuciferase (siGL transfected).

Figure S5. Plk1 is required for proper primary cilia disassembly throughout the cell cycle. (A, B) hTERT-RPE cells were infected with sh-lentiviruses to silence either control luciferase (shGL) or Plk1 (shPlk1). Forty-eight hours after serum starvation, the cells were stimulated with serum and harvested at the indicated time points. The resulting samples were subjected to immunostaining analyses to quantify the fraction of cells with primary cilia **(A top, actual fraction of cells with primary cilia; A bottom, relative number of cells with primary cilia replotted from A top)** and flow cytometry analyses to monitor the cell cycle progression (**B**). More than 300 cells were counted for each sample from three independent experiments. Error bars, standard deviations. Notably, a significant defect in primary cilia disassembly in shPlk1 cells was apparent ~4-6 h after serum stimulation. On the other hand, a delay in the cell cycle in shPlk1 cells was not readily observed until 12-18 h after the stimulation {judging from the appearance of G2/M peak (arrows)}. These findings suggest that a defect in primary cilia disassembly may have caused the late stage cell cycle delay in shPlk1 cells. Y-axis indicates cell numbers, while X-axis denotes DNA content revealed by propidium iodide staining. 2N, 2N DNA content; 4N, 4N DNA content. Bars, standard deviation. Note that depletion of Plk1 appears to steadily delay primary cilia disassembly from as early as a few hours after serum stimulation.

Figure S6. **Requirement of Plk1 activity for proper disassembly of primary cilia in hTERT-RPE cells. (A–C)** hTERT RPE cells serum-starved for 48 h were treated with control DMSO or Plk1 inhibitor, BI 2536, 2 h prior to serum stimulation. Cells were fixed at the indicated time points after serum stimulation, immunostained **(A)**, and quantified **(B)**. A fraction of the same cells was subjected to flow cytometry analyses to monitor cell cycle progression **(C)**. Representative cells at 0 h and 18 h after serum stimulation (2 h and 20 h, respectively, after the compound treatment) are shown in **(A)**. AurA inhibitor (VX-680) was included for comparison. Error bars in **(B)** indicate standard deviation from more than three independent experiments. 2N, 2N DNA content; 4N, 4N DNA content. Note that BI 2536 effectively impaired proper cilia disassembly, even though it did not induce mitotic arrest as potently as the AurA inhibitor, VX-680, in **(C)**.

Figure S7. Replotted data of the results in Figure 4C–D to determine the relative efficiency of primary cilia disassembly. The relative number of cells with primary cilia **(A)** and relative length of primary cilia **(B)** were calculated by determining values proportional to the values in the 0 h sample in each group. Error bars, standard deviation relative to the 0 h samples in each group.

Figure S8. Interactions between Plk1 PBD and the p-S143 and p-T224 epitopes of Dvl2 under serum-starved and -stimulated conditions. (A) Total lysates prepared from 48 h serum-starved hTERT-RPE cells were subjected to pull-downs with bead-

immobilized control GST, GST-PBD wild-type (WT), or GST-PBD (H538A K540M) (AM). Precipitates were treated with λ phosphatase (λ PPase) and then subjected to immunoblotting analyses. The resulting membrane was stained with Coomassie (CBB). Numbers for the 0 h and 3 h pull-down samples are the signal intensities relative to those in the input. Note that serum stimulation for 3 h enhances the PBD-Dvl2 interaction approximately 5 fold in comparison to the basal level of interaction under serum starvation conditions (0 h) **(B)** hTERT-RPE cells were transfected with the indicated Dvl2 constructs. Twenty-four hours after transfection, cells were serum-starved for 48 h, and then subjected to PBD pull-downs.

Figure S9. Defect in primary cilia disassembly in cells expressing shDvl2-insensitive S143A or T224A mutant. (A) hTERT-RPE cells expressing the indicated sh-insensitive Dvl2 constructs were infected with appropriate lentiviruses to silence either control luciferase (shGL) or endogenous Dvl2 (shDvl2). The resulting cells were grown asynchronously and then immunoblotted to determine the level of exogenous Dvl2 expression. The asterisk indicates a degradation product of exogenous Dvl2. **(B)** The same cells in (**A**) were starved for 48 h, stimulated with serum, and then fixed at the indicated time points after serum stimulation. The resulting samples were immunostained with acetylated tubulin antibody and the cells with primary cilia were quantified. Note that similar results were obtained with the Dvl2 mutants partially sensitive to shDvl2 (see **Figure 4E** and **4F** for details). >300 cells were counted from each sample. Error bars, standard deviation from multiple independent experiments. **(C)** HEK293T cells transfected with the indicated Dvl2 constructs were subjected to PBD pull-downs, and

immunoblotted. Numbers, relative amounts of Dvl2 bound to GST-PBD. Note that mutation of S143 or T224 to a negatively charged residue (**D** or **E**) significantly cripples the ability of Dvl2 to bind to GST-PBD.

Figure S10. Differential localization of CK1δ and CK1ε at mitotic centrosomes. (A, B) Forty-eight hours after serum starvation, hTERT-RPE cells were stimulated with serum for 18 h. The resulting cells were then briefly extracted with 0.5% Triton X-100 and fixed. The resulting cells were immunostained with the indicated antibodies **(A)** and centrosomal fluorescence intensities were quantified **(B**) (see also **Figure 5E** and **F** for interphase centrosome-localized CK1δ and CK1ε signals). Greater than 300 cells were counted from each sample. Bars, standard deviation.

Figure S11. Requirement of CK1ε in Wnt5a-dependent primary cilia disassembly. (**A)** hTERT-RPE cells were depleted of either endogenous CK1δ or CK1ε, serum-starved for 48 h, and treated with control or Wnt5a CM for 1 h prior to serum stimulation. The cells were fixed according to the schedule in Figure 6B, immunostained, and quantified. Note that treatment of cells with Wnt5a CM promoted primary cilia disassembly in both shLuciferase (shGL) and shCK1δ cells. In contrast, Wnt5a treatment failed to significantly enhance this process upon depletion of CK1ε (shCK1ε). Greater than 300 cells were counted for each sample. Bars, standard deviation. **(B)** To examine the level of Wnt5a expression during ciliary disassembly process, hTERT-RPE cells were serum-starved for 48 h, stimulated with serum, and then harvested at the indicated time points after stimulation. The cells were lysed in TBSN {20 mM Trish-Cl (pH 8.0), 150 mM

NaCl, 0.5% NP-40, 5 mM EGTA, 1.5 mM EDTA, 20 mM *p*-nitrophenylphosphate and protease inhibitor cocktail (Roche)} buffer, centrifuged, and the resulting supernatants were subjected to immunoblotting analyses. Asterisk, cross-reacting protein.

Figure S12. The Dvl2-Plk1 complex regulates HEF1 stability, but not HEF1 transcription. (A) To examine whether depletion of Dvl2 or disruption of the Dvl2-Plk1 interaction alters the level of HEF1 mRNA, hTERT-RPE cells expressing the indicated constructs were silenced for either control luciferase (shGL) or Dvl2 (shDvl2), and then serum-starved for 48 h. Following serum stimulation, cells were harvested at indicated time points using TRIzol. Total RNA purified from the respective samples was subjected to semi-quantitative RT-PCR using specific primers for HEF1 and β-actin mRNAs. **(B)** Total lysates from the 2.5 h samples in **(A)** were immunoblotted, and then stained with Coomassie (CBB). Numbers indicate relative amount of HEF1. **(C)** hTERT-RPE cells were serum-starved for 48 h and then treated with either control DMSO or BI 2536 2 h prior to serum stimulation. Where indicated, the resulting cells were additionally treated with cycloheximide (CHX) 2 h after serum stimulation to inhibit protein synthesis. Cells were harvested at the indicated time points and subjected to immunoblotting analyses. Numbers indicate relative amounts of HEF1 in each sample. The levels of p-Erk1/2 serve as loading controls.

Figure S13. HEF1 protein stability is regulated by the reciprocal binding of Smad3 to HEF1 or to the Dvl2-Plk1 complex. (A–E) Plk1 does not appear to regulate the HEF1 stability by direct phosphorylation. **(A)** HeLa cells transfected with Flag-HEF1

were treated with thymidine or nocodazole for 18 h before harvest. The resulting cells were immunoprecipitated and separated by SDS-PAGE. The Flag-HEF1 band was excised from the gel and analyzed by mass spectrometry to determine *in vivo* phosphorylation sites. **(B)** Bacterial purified GST-HEF1 was reacted with insect Flag-Plk1 WT or the respective kinase-inactive K82M mutant. Samples were separated by SDS-PAGE, stained with Coomassie (CBB), and autoradiographed. Similar reactions were carried out in the presence of excess ATP to determine Plk1-dependent HEF1 phosphorylation sites by mass spectrometry analyses. **(C)** Seven overlapped phosphopeptides from **(A)** and **(B)** are shown. Phosphosites are marked with asterisks. **(D)** hTERT-RPE cells expressing Flag-HEF1 WT or the respective 7A mutant were depleted of endogenous HEF1. The resulting cells were serum-starved for 48 h and treated with 10 μM MG132 for 2 h prior to serum stimulation. Cells harvested 3 h after serum stimulation were subjected to immunoprecipitation and immunoblotting analyses. Because of the interaction between Smad3 and Smad2, co-precipitated Smad2 is detected in the immunoblot with anti-Smad2/3 antibody. **(E)** The cells in **(D)** were serum-starved for 48 h and then treated with both serum and cycloheximide (CHX) at the same time. Cells were harvested at the indicated time points and subjected to immunoblotting analyses. The level of α-tubulin serves as a loading control. **(F)** Reciprocal binding of Smad3 to HEF1 or to Dvl2. Serum-starved hTERT-RPE cells were treated 10 μM MG132 together with either DMSO, 200 nM BI 2536 or 50 μM IC261 for 2 h prior to serum stimulation. The resulting cells were harvested 3 h after serum stimulation and subjected to immunoprecipitation analyses. Note that Smad2 is also detected in the

Smad3 immunoprecipitates because of the interaction between these two proteins. Numbers, relative efficiencies of co-immunoprecipitation.

Figure S14. Localization of endogenous CK1ε and Dvl2 to ciliary basal bodies and direct interaction between CK1ε and Dvl2 *in vitro*. (**A)** To examine whether endogenous CK1ε and Dvl2 localize to ciliary basal bodies, hTERT-RPE cells were serum-starved for 48 h. The cells were then immunostained with the indicated antibodies after extraction with 0.5% Triton X-100. Primary cilia were detected with antibodies against either acetylated or glutamylated tubulin. **(B)** Bead-immobilized, purified bacterial control GST or GST-CK1ε was incubated with HEK293T cell lysates expressing Flag-Dvl2, and then subjected to pull-down assays. Precipitates were immunoblotted and the resulting membrane was stained with Coomassie (CBB).

Figure S15. Differential effect of Dvl2 knockdown between ciliated hTERT-RPE cells and non/less-ciliated HeLa cells during cell cycle progression. (A) hTERT-RPE cells were silenced for either control luciferase (shGL) or Dvl2 (shDvl2), and then serum-starved for 48 h. Upon completion of starvation, a set of samples were fixed and immunostained to determine the efficiency of primary cilia formation in G0 interphase cells. Another set of samples were prepared after serum stimulation for 24 h, and then immunostained to examine the frequency of primary cilia formation in mitotic cells. Note that none of the mitotic hTERT-RPE cells (> 300 cells) exhibited primary cilia under shGL or shDvl2-treated conditions, suggesting that primary cilia disassembly is required prior to mitotic entry. **(B)** To comparatively examine the phenotypes associated with

Dvl2 depletion in HeLa and hTERT-RPE cells, the respective cells were silenced for either control luciferase (shGL) or Dvl2 (shDvl2), and then subjected to immunostaining analyses. Both mitotic indices and the fraction of mitotic cells with multipolar spindles (≥3 centrosomes) were quantified. Representative images are shown **(right)**. Interestingly, depletion of Dvl2 induced mitotic arrest with multipolar spindles in HeLa cells. In contrast, it rather diminished mitotic index in hTERT-RPE cells with no detectable spindle defect. The apparent differences observed between HeLa and hTERT-RPE cells could be in part attributable to the fact that the majority (>95%) of HeLa cells do not bear detectable primary cilia. In addition, failure to detect multipolar spindles even in mitotic hTERT-RPE shDvl2 cells suggests that these cells may have a tighter regulation in the establishment of bipolar spindles. For both **(A)** and **(B)**, greater than 300 cells were counted from each sample. Bars, standard deviation.

Lee KH, et al., Fig. S1

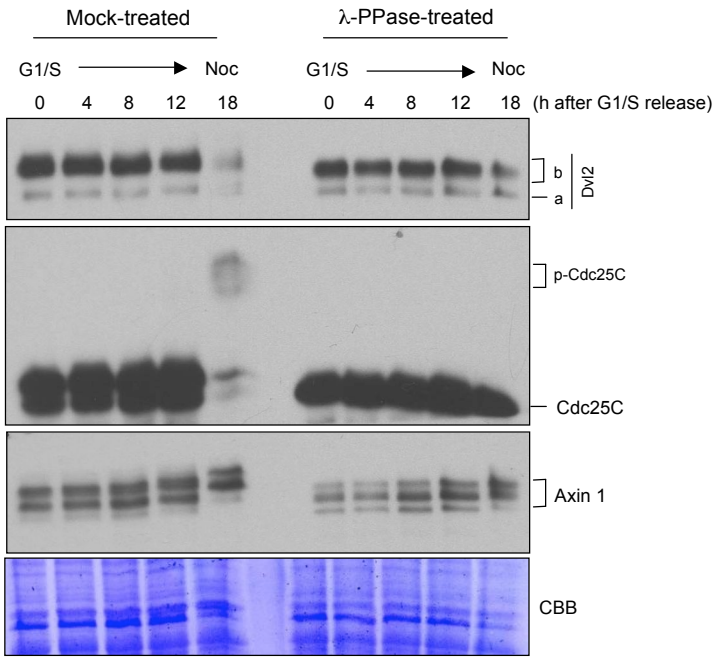

A

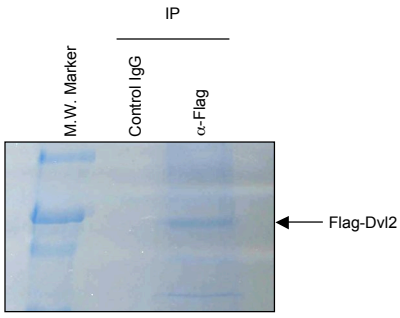
IP
M.W. Marker
Control IgG
α-Flag
Flag-Dvl2

B

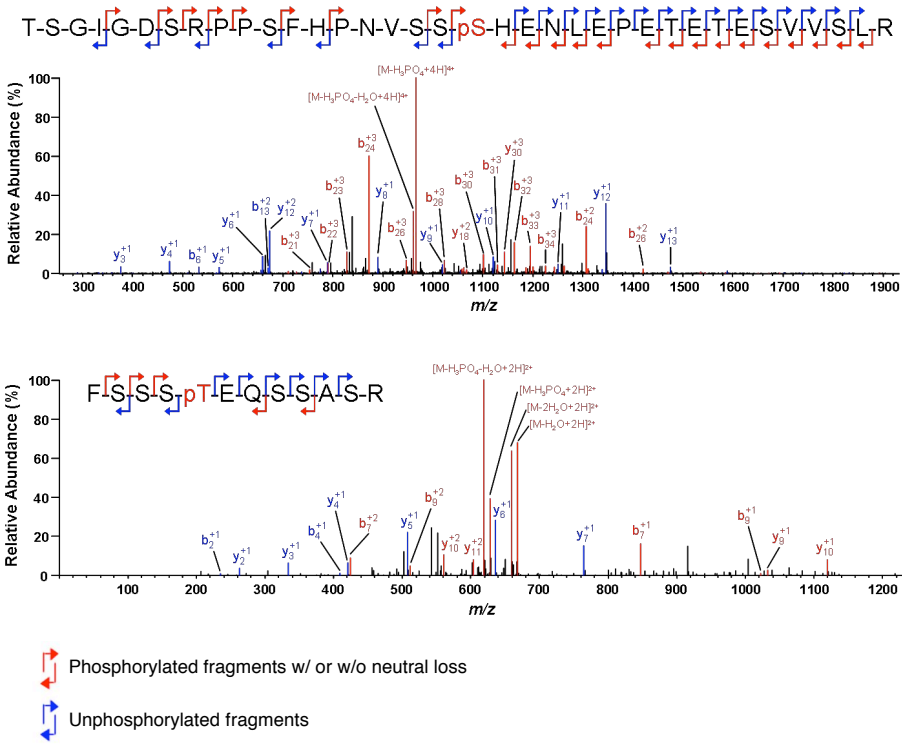
T-S-G-I-G-D-S-R-P-P-S-F-H-P-N-V-S-S-pS-H-E-N-L-E-P-E-T-E-T-E-S-V-V-S-L-R
Relative Abundance (%)
m/z
F-S-S-S-pT-E-Q-S-S-A-S-R
Relative Abundance (%)
m/z
Phosphorylated fragments w/ or w/o neutral loss
Unphosphorylated fragments

C

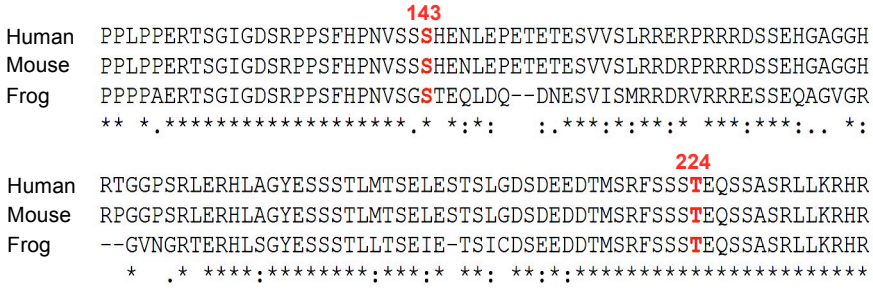

D

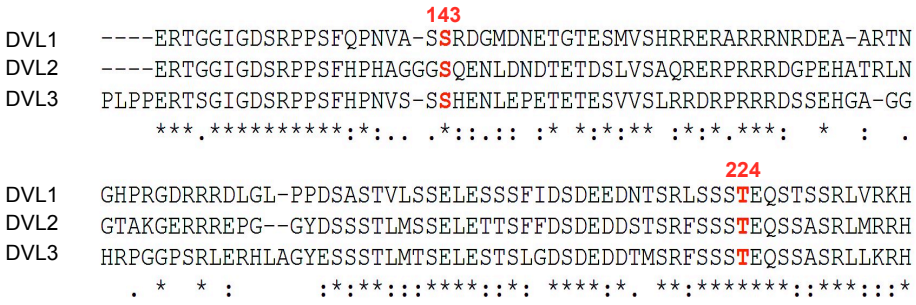

E

In vitro kinase reaction	Peptides identified (Asterisks indicate phospho-residues)	Regions	Frequency
Ck1δ + Dvl2			
S143 site	R.TSGIGDSRPPSFHPNVSS**S***HENLEPETETESVVSLR.R	124 - 161	4
T224 site	R.FSSS**T***EQSSASR.L	219 - 232	9
	R.FSSS**T***EQSSASRLLKR.H	219 - 236	2
Ck1ε + Dvl2			
S143 site	R.TSGIGDSRPPSFHPNVSS**S***HENLEPETETESVVSLR.R	124 - 161	4
T224 site	R.FSSS**T***EQSSASR.L	219 - 232	2

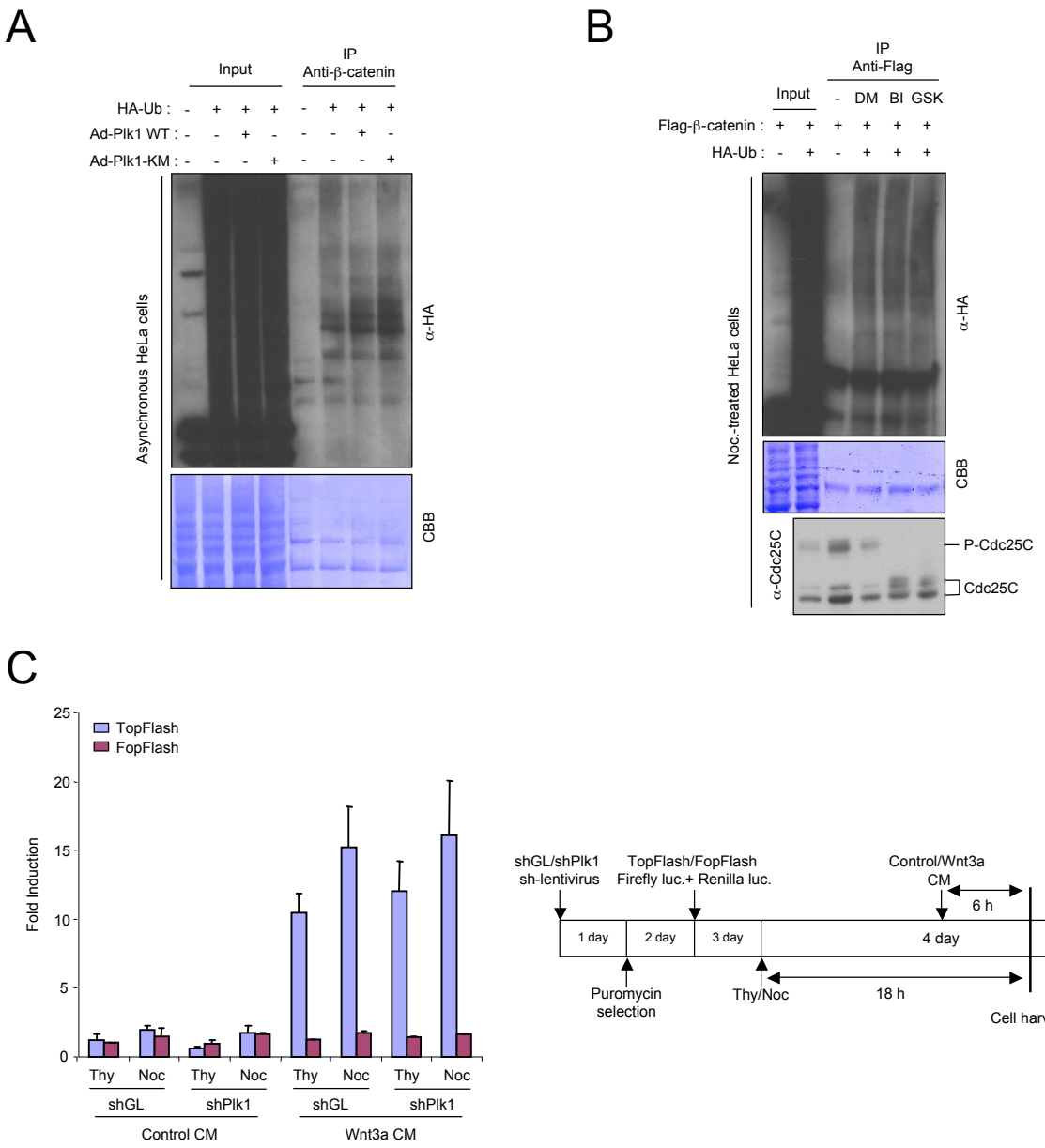
A
Input
IP
Anti-β-catenin
HA-Ub : - + + + - + + +
Ad-Plk1 WT : - - + - - - + -
Ad-Plk1-KM : - - - + - - - +
Asynchronous HeLa cells
α-HA
CBB
B
IP
Anti-Flag
Input
- DM BI GSK
Flag-β-catenin : + + + + + +
HA-Ub : - + - + + +
Noc.-treated HeLa cells
α-HA
CBB
α-Cdc25C
P-Cdc25C
Cdc25C
C
TopFlash
FopFlash
Fold Induction
25
20
15
10
5
0
Thy Noc Thy Noc Thy Noc Thy Noc
shGL shPlk1 shGL shPlk1
Control CM
Wnt3a CM
shGL/shPlk1
sh-lentivirus
TopFlash/FopFlash
Firefly luc.+ Renilla luc.
Control/Wnt3a
CM
6 h
1 day
2 day
3 day
4 day
Puromycin
selection
Thy/Noc
18 h
Cell harvest

A

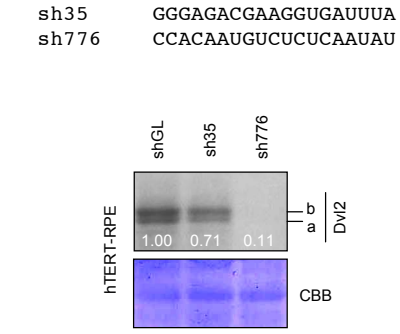
sh35 GGGAGACGAAGGUGAUUUA
sh776 CCACAAUGUCUCUCAAUAU
shGL
sh35
sh776
hTERT-RPE
1.00
0.71
0.11
b
a
Dvl2
CBB

B

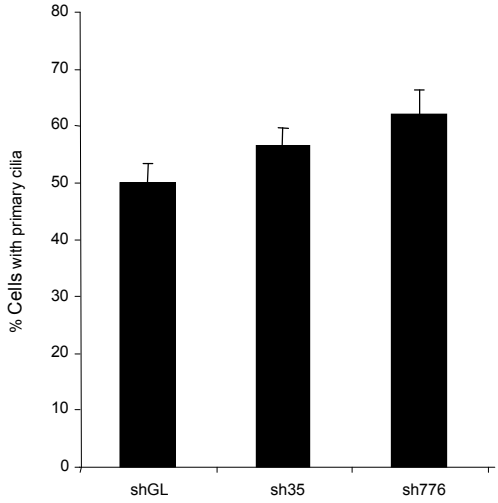
% Cells with primary cilia
80
70
60
50
40
30
20
10
0
shGL
sh35
sh776

C

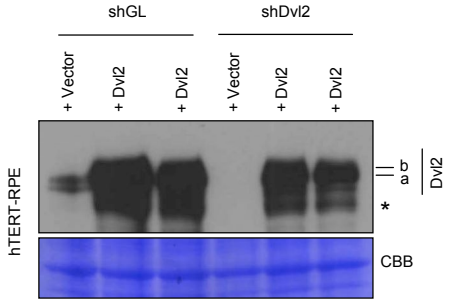
shGL
shDvl2
+ Vector
+ Dvl2
+ Dvl2
+ Vector
+ Dvl2
+ Dvl2
hTERT-RPE
b
a
Dvl2
*
CBB

D

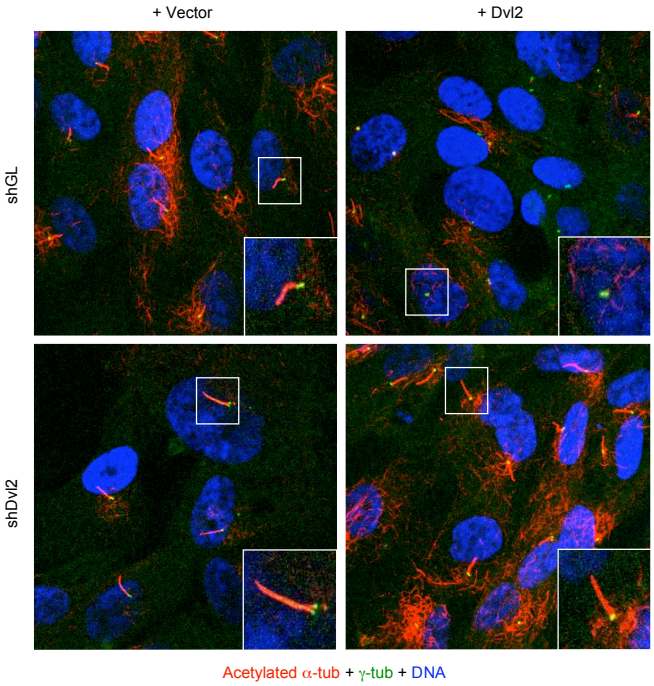
+ Vector
+ Dvl2
shGL
shDvl2
Acetylated α-tub + γ-tub + DNA

E

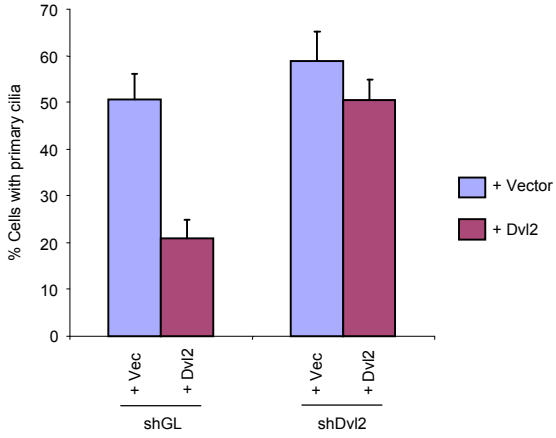
% Cells with primary cilia
70
60
50
40
30
20
10
0
+ Vec
+ Dvl2
shGL
shDvl2
+ Vector
+ Dvl2

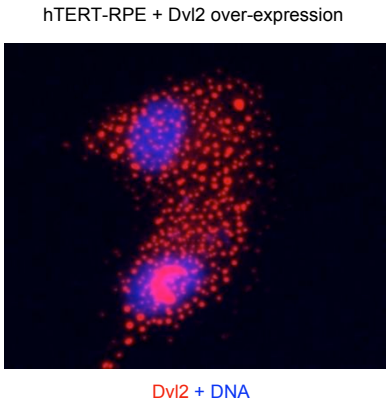
hTERT-RPE + Dvl2 over-expression
Dvl2 + DNA

F

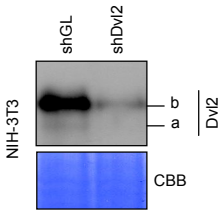
shGL
shDvl2
NIH-3T3
b
a
Dvl2
CBB

G

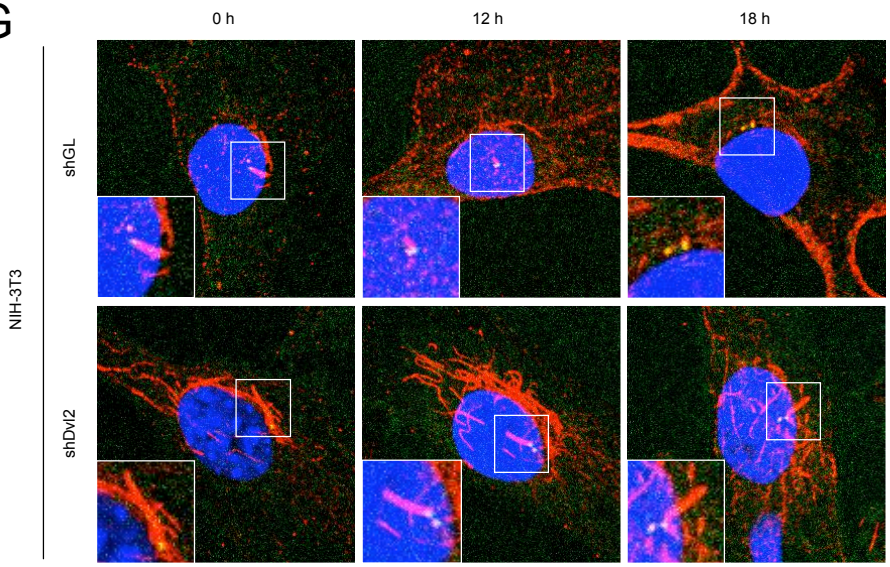
0 h
12 h
18 h
shGL
shDvl2
NIH-3T3
Acetylated α-tub + γ-tub + DNA

H

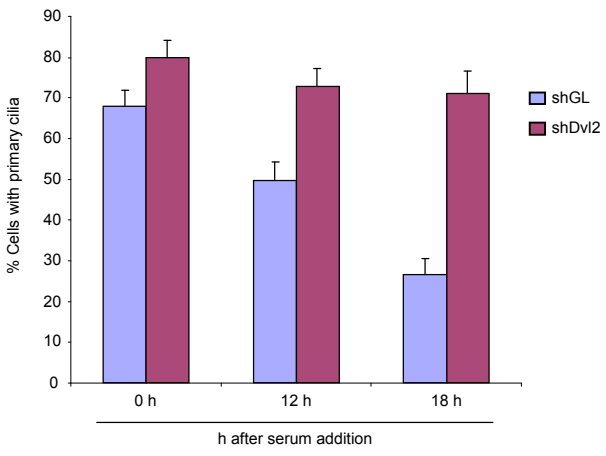
% Cells with primary cilia
90
80
70
60
50
40
30
20
10
0
0 h
12 h
18 h
h after serum addition
shGL
shDvl2

I

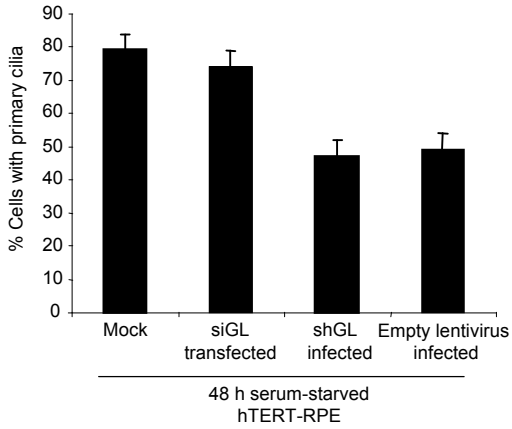
% Cells with primary cilia
90
80
70
60
50
40
30
20
10
0
Mock
siGL transfected
shGL infected
Empty lentivirus infected
48 h serum-starved hTERT-RPE

Lee KH, et al., Fig. S5

A

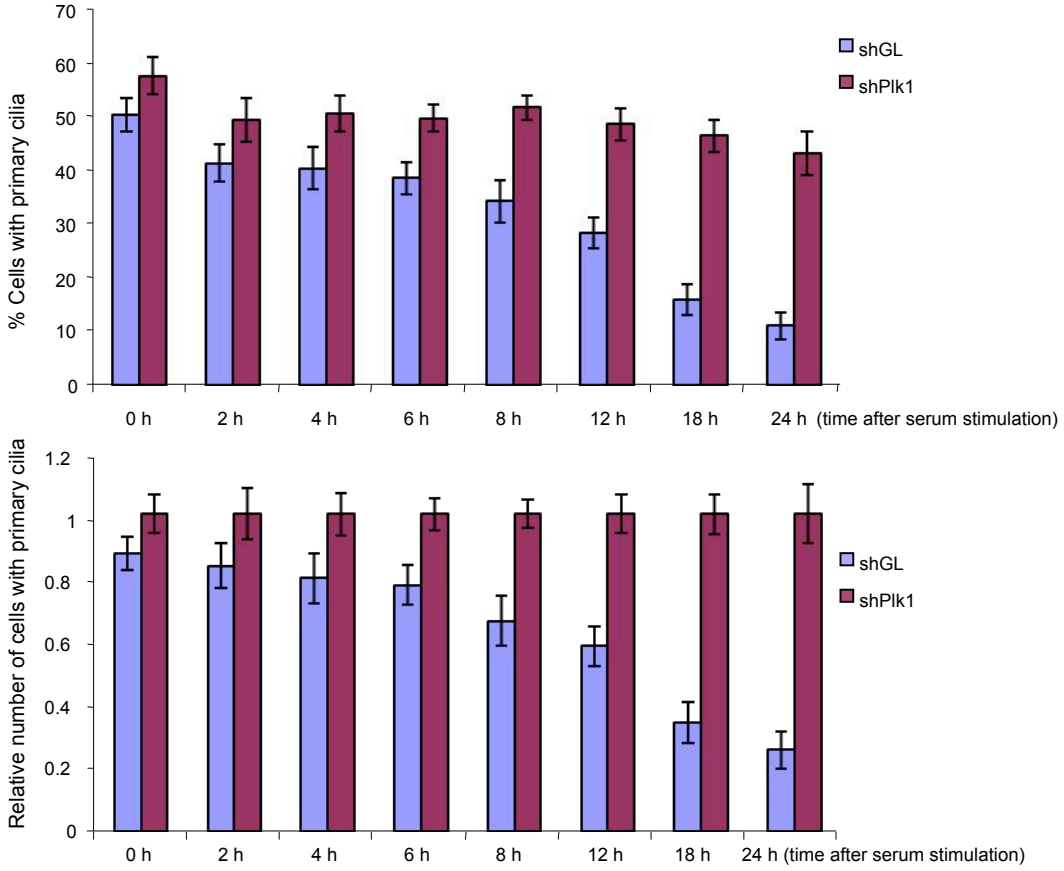

B

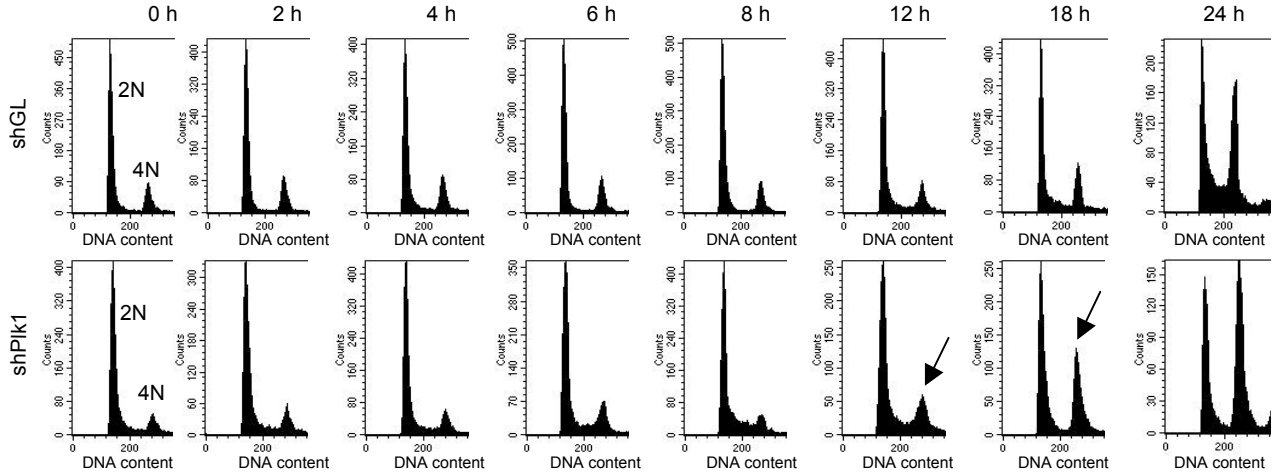

Lee KH, et al., Fig. S6

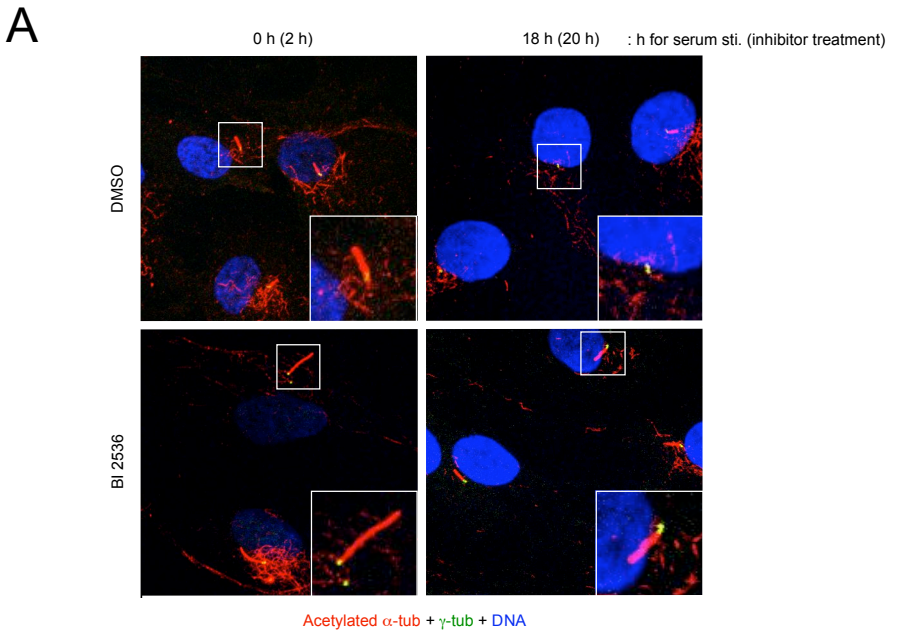

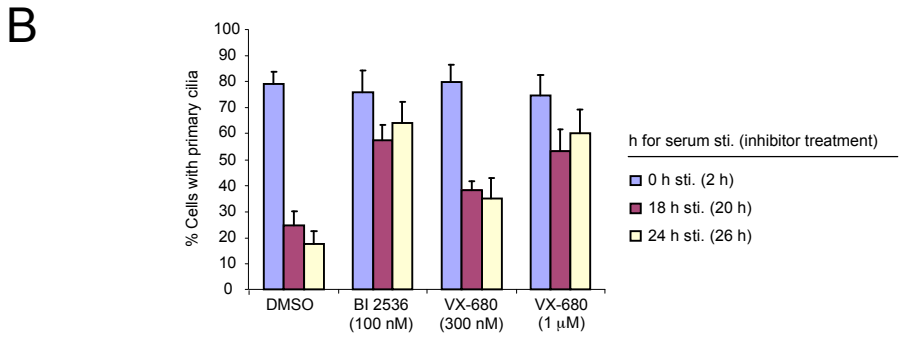

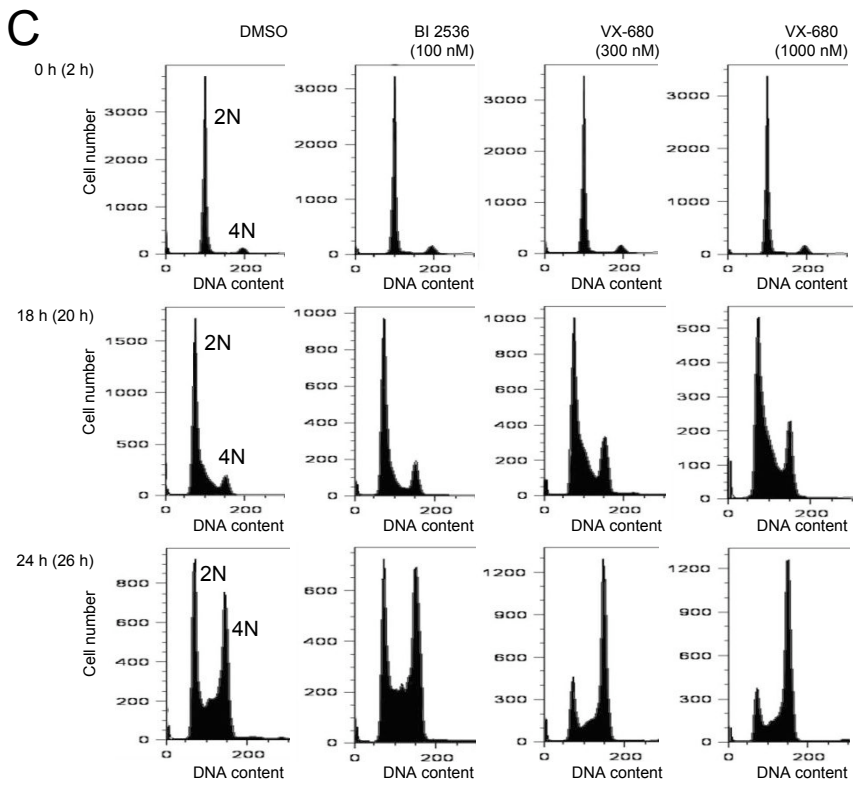

Lee KH, et al., Fig. S7

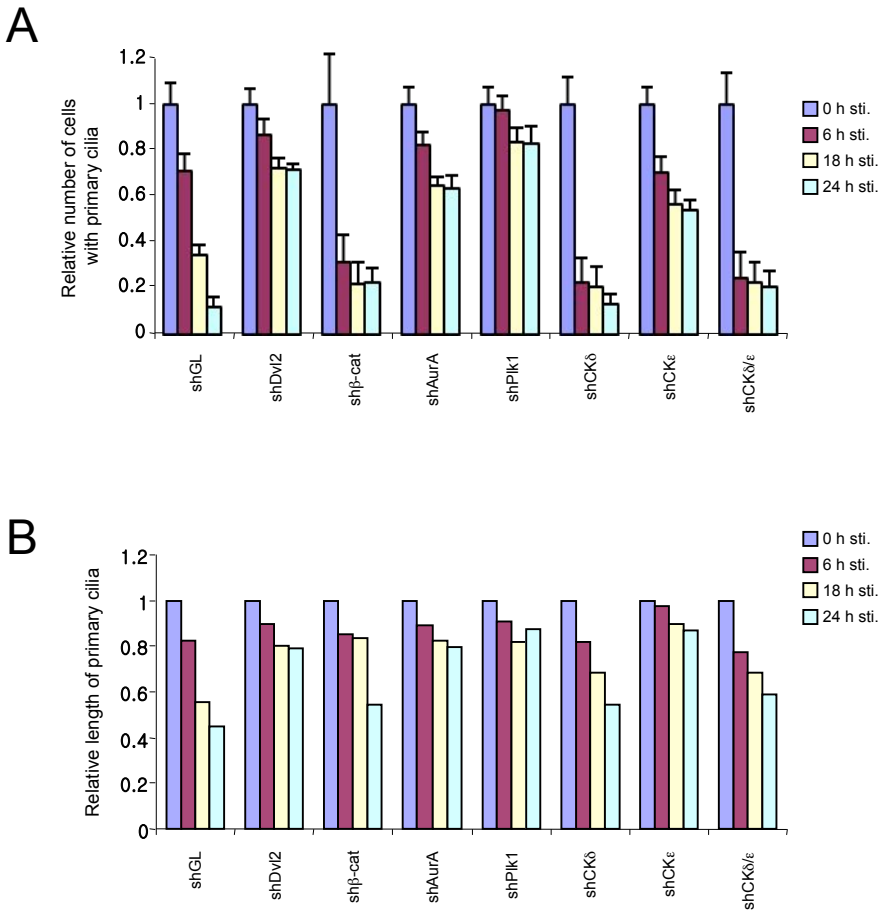

Lee KH, et al., Fig. S8

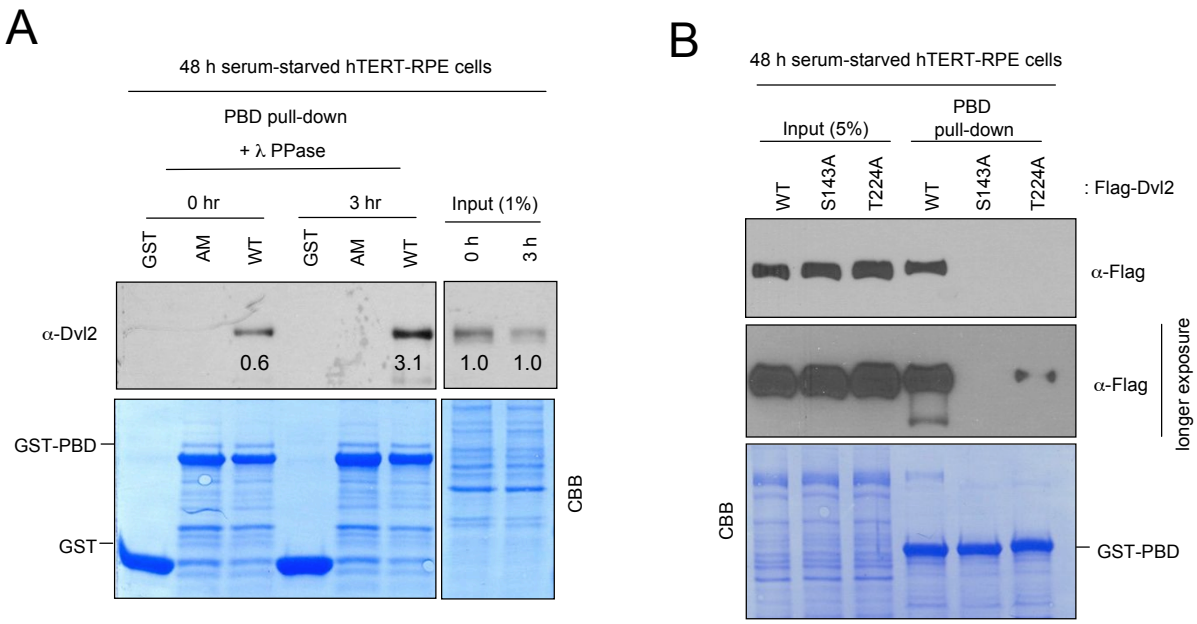

A

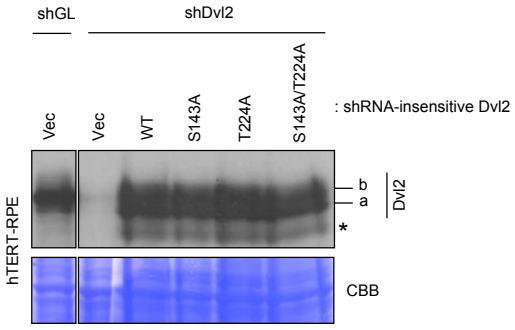
shGL
shDvl2
Vec
Vec
WT
S143A
T224A
S143A/T224A
: shRNA-insensitive Dvl2
hTERT-RPE
b
a
Dvl2
*
CBB

B

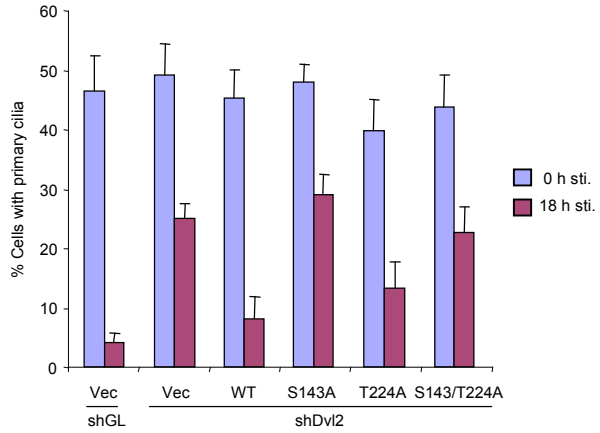
% Cells with primary cilia
60
50
40
30
20
10
0
Vec
Vec
WT
S143A
T224A
S143/T224A
shGL
shDvl2
0 h sti.
18 h sti.

C

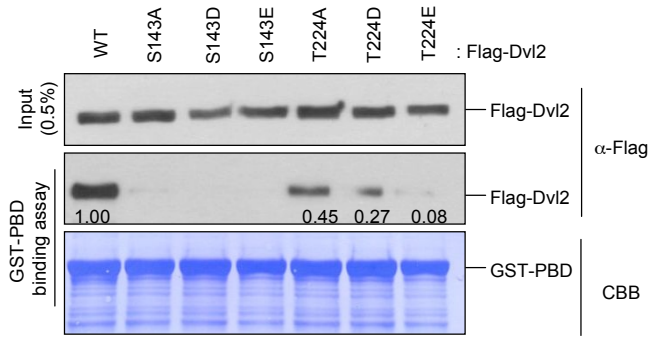
WT
S143A
S143D
S143E
T224A
T224D
T224E
: Flag-Dvl2
Input (0.5%)
Flag-Dvl2
α-Flag
GST-PBD binding assay
Flag-Dvl2
1.00
0.45
0.27
0.08
GST-PBD
CBB

Lee KH, et al., Fig. S10

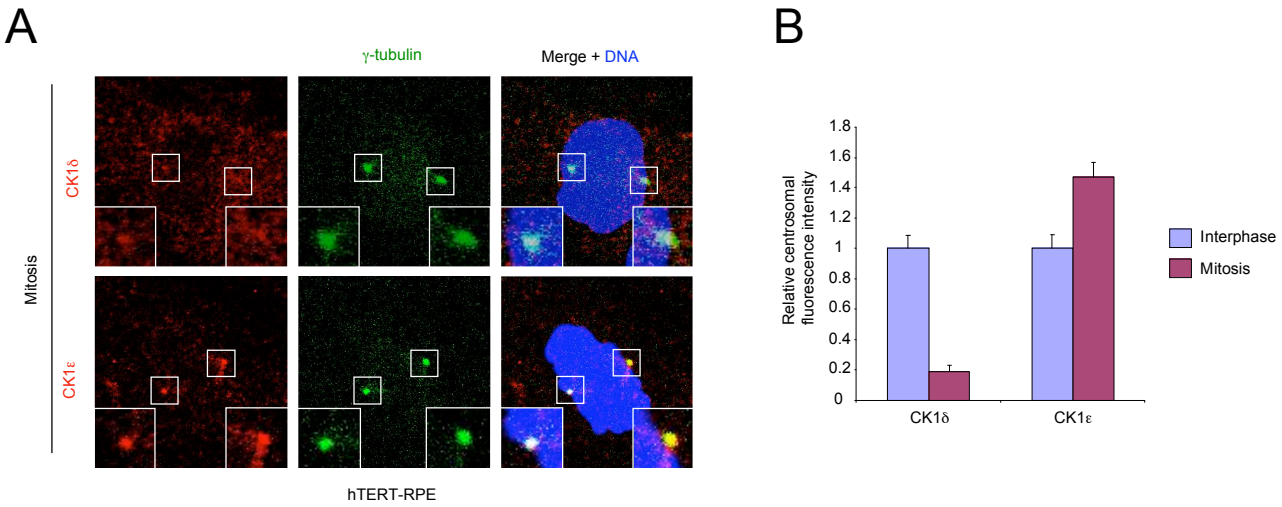

A

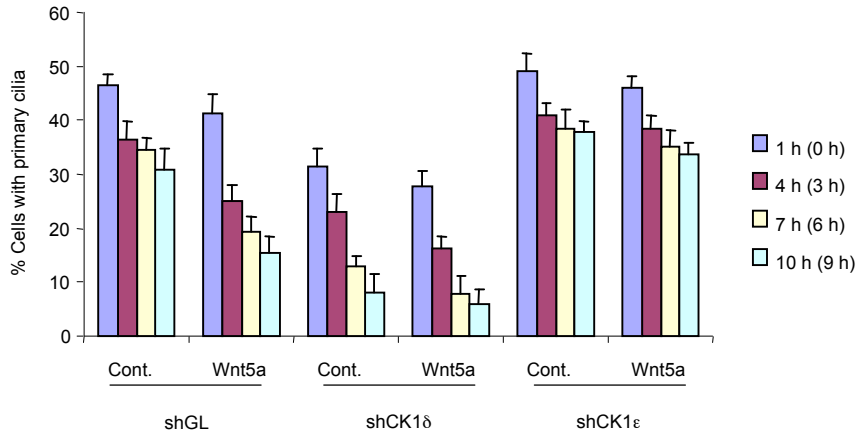
% Cells with primary cilia
60
50
40
30
20
10
0
Cont.
Wnt5a
Cont.
Wnt5a
Cont.
Wnt5a
shGL
shCK1δ
shCK1ε
1 h (0 h)
4 h (3 h)
7 h (6 h)
10 h (9 h)

B

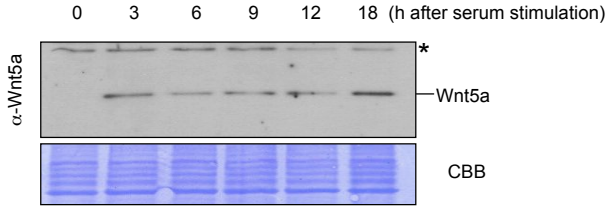
0 3 6 9 12 18 (h after serum stimulation)
α-Wnt5a
*
Wnt5a
CBB

Lee KH, et al., Fig. S12

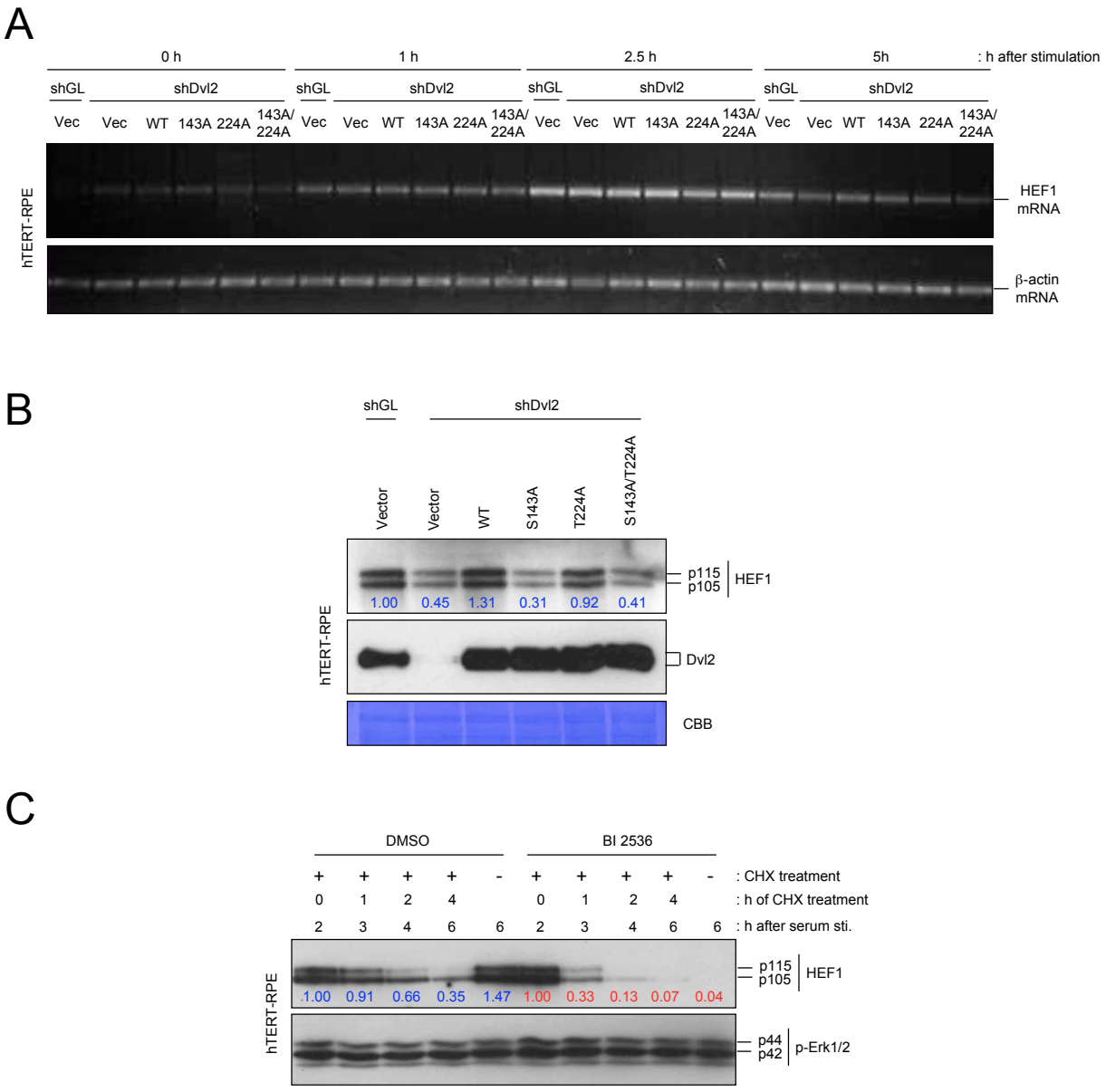

A

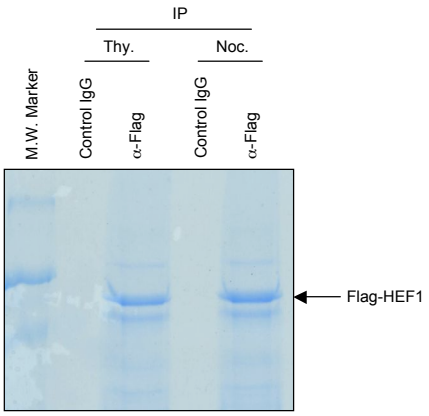

B

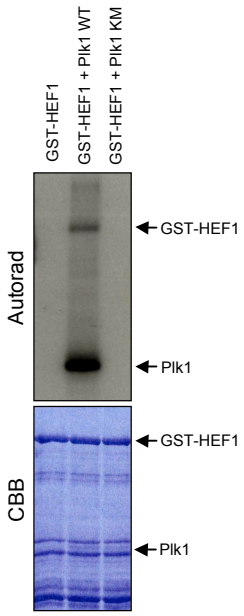

C

Peptides identified	Phosphosites
R.KGDILTVIEQNTGGLEGWWLC**S***LHGR.Q	S47
R.VEDSHQILSQTSHDLNEC**S***WSLNILAINKPQNK.C	S510
K.QL**T***TTINTNAEALFR.P	T546
K.QLTT**T***INTNAEALFR.P	T548
K.QLTTTIN**T***NAEALFR.P	T551
K.EQAPDC**S***SSDGSER.S	S616
K.VMNS**S***NQLCEQLK.T	S780

Asterisks indicate phosphorylated residues.

D

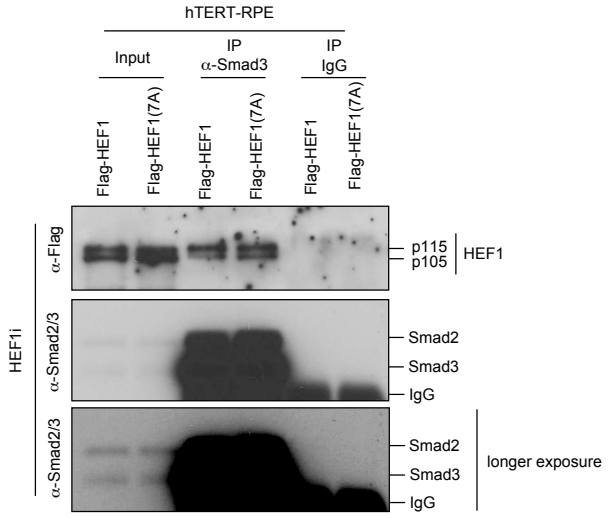
hTERT-RPE
Input
IP α-Smad3
IP IgG
Flag-HEF1
Flag-HEF1(7A)
HEF1i
α-Flag
α-Smad2/3
p115
p105
HEF1
Smad2
Smad3
IgG
longer exposure

E

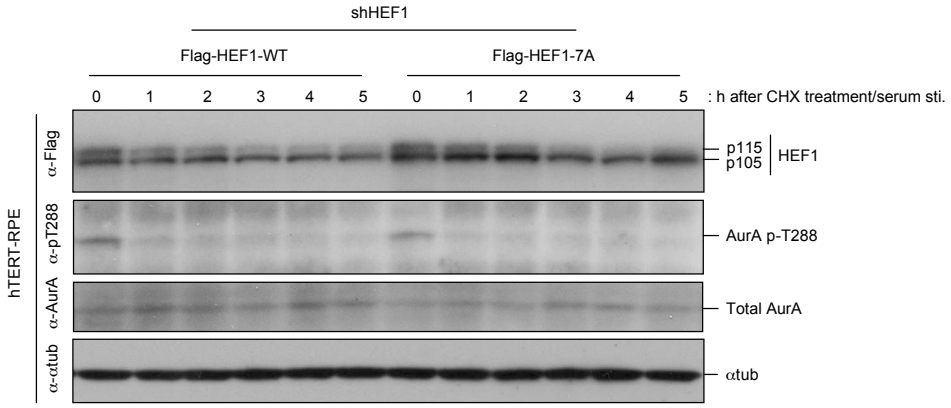
shHEF1
Flag-HEF1-WT
Flag-HEF1-7A
0 1 2 3 4 5 0 1 2 3 4 5
: h after CHX treatment/serum sti.
hTERT-RPE
α-Flag
α-pT288
α-AurA
α-αtub
p115
p105
HEF1
AurA p-T288
Total AurA
αtub

F

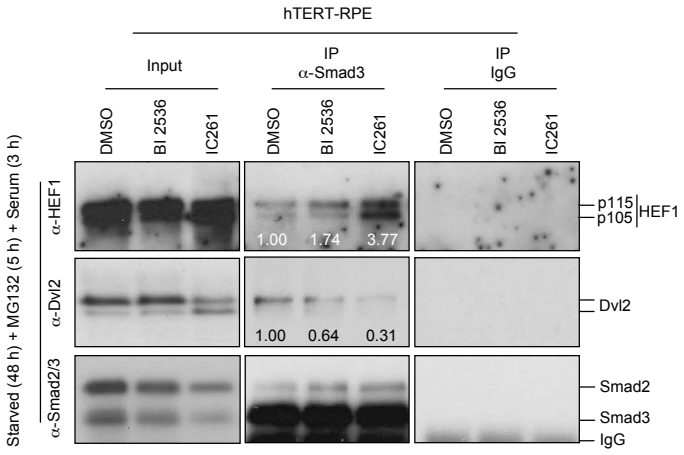
hTERT-RPE
Input
IP α-Smad3
IP IgG
DMSO
BI 2536
IC261
Starved (48 h) + MG132 (5 h) + Serum (3 h)
α-HEF1
α-Dvl2
α-Smad2/3
1.00 1.74 3.77
1.00 0.64 0.31
p115
p105
HEF1
Dvl2
Smad2
Smad3
IgG

A

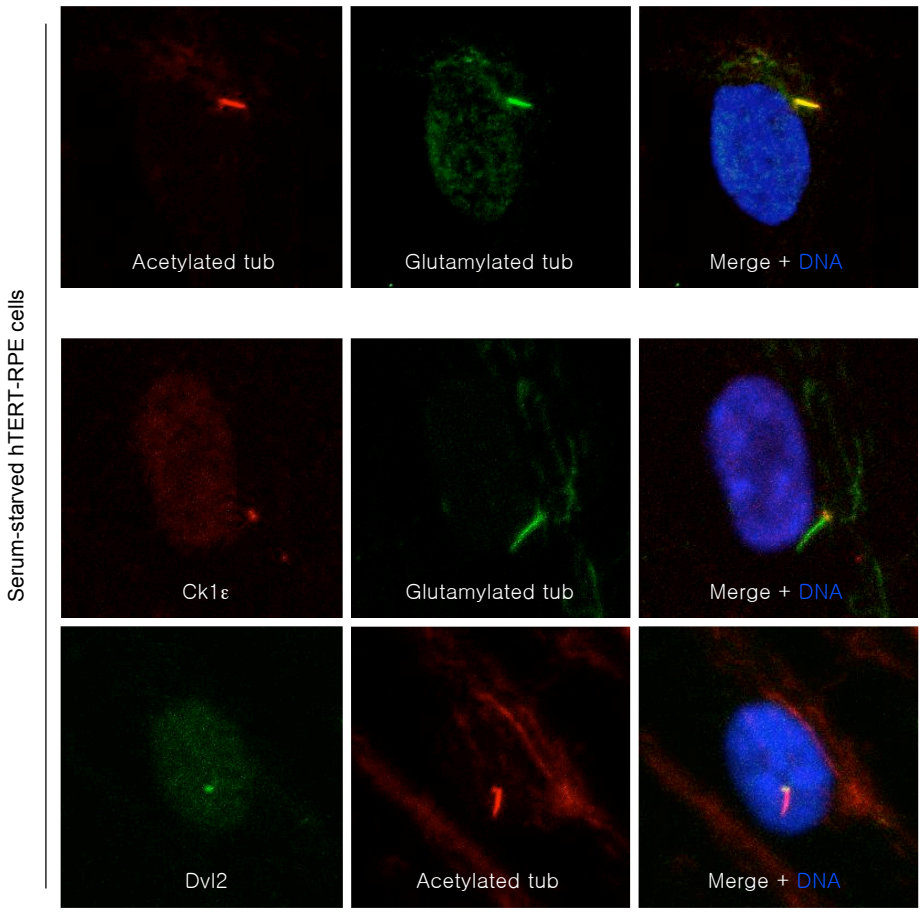
Serum-starved hTERT-RPE cells
Acetylated tub
Glutamylated tub
Merge + DNA
Ck1ε
Glutamylated tub
Merge + DNA
Dvl2
Acetylated tub
Merge + DNA

B

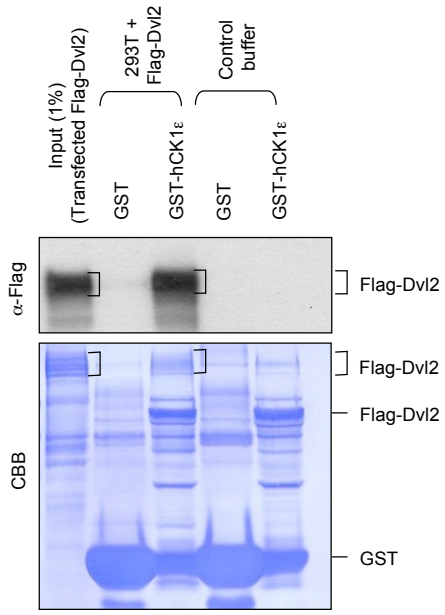
Input (1%)
(Transfected Flag-Dvl2)
293T + Flag-Dvl2
Control buffer
GST
GST-hCK1ε
GST
GST-hCK1ε
α-Flag
Flag-Dvl2
CBB
Flag-Dvl2
Flag-Dvl2
GST

A

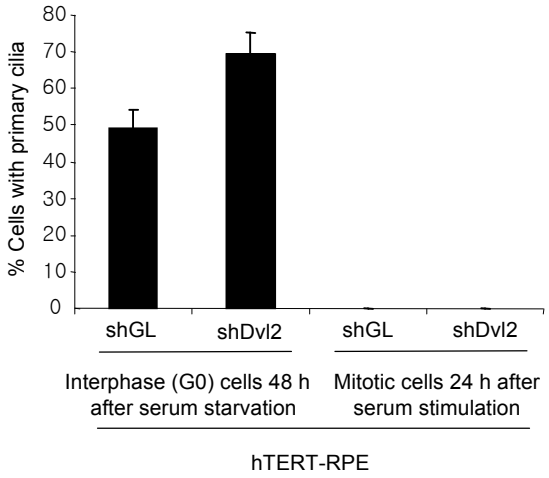
% Cells with primary cilia
80
70
60
50
40
30
20
10
0
shGL
shDvl2
shGL
shDvl2
Interphase (G0) cells 48 h after serum starvation
Mitotic cells 24 h after serum stimulation
hTERT-RPE

B

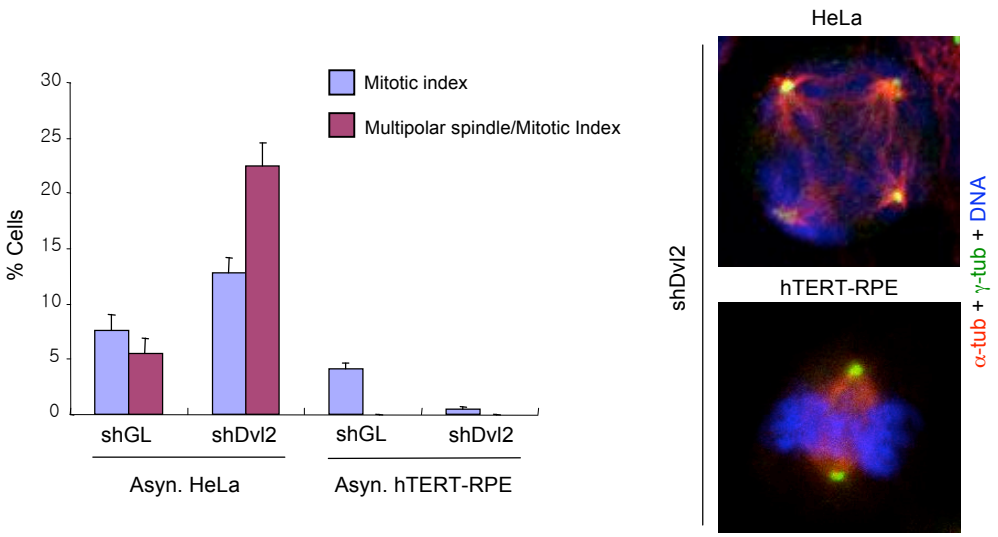
Mitotic index
Multipolar spindle/Mitotic Index
% Cells
30
25
20
15
10
5
0
shGL
shDvl2
shGL
shDvl2
Asyn. HeLa
Asyn. hTERT-RPE
HeLa
shDvl2
hTERT-RPE
α-tub + γ-tub + DNA

Table S1. Sequences of siRNAs used in this study

Target	Sense strand (5' -> 3')	Position (nt from start codon)	Source	References
Dvl2	CCACAATGTCTCTCAATAT	776-794	Lentivirus	This study
Plk1	AGATTGTGCCTAAGTCTCT	245-263	Lentivirus, synthetic	Hansen et al., 2004
Aurora A	ATGCCCTGTCTTACTGTCA	725-743	Lentivirus	Pugacheva et al., 2007
β-catenin	GGATGTTCACAACCGAATTGTTAT	1746-1769	Lentivirus	Perez-Ruiz et al., 2008
Ck1δ	AGGCTACCCTTCCGAATTT	726-744	Lentivirus	This study
Ck1ε	GATCAGCCGCATCGAGTAT	336-354	Lentivirus	This study
HEF1	CCATGAGACAAGCTGGAAGGC	737-757	Lentivirus	Dadke et al., 2006
Luciferase	CGTACGCGGAATACTTCGA		Lentivirus, synthetic	Elbashir et al., 2001
Ck1α Ck1γ1 Ck1γ2 Ck1γ3	ON-TARGETplus SMARTpool (Dharmacon)			

nt: nucleotide

Table S2. Antibodies Used in this Study

Antibodies	Host Species	Source
anti-Dvl2	rabbit	Cell Signaling, Danvers, MA
anti-Dvl2 p-S143	rabbit	This study
anti-Dvl2 p-T224	rabbit	This study
anti-Plk1	rabbit/mouse	Lab stock/SantaCruz, Santa Cruz, CA
Anti-Cdc25C	rabbit	SantaCruz, Santa Cruz, CA
anti-CK1δ	mouse	SantaCruz, Santa Cruz, CA
anti-CK1ε	mouse	BD Transduction Lab. Franklin Lakes, NJ
anti-β-catenin	mouse	BD Transduction Lab. Franklin Lakes, NJ
anti-Aurora A	rabbit	Cell Signaling, Danvers, MA
anti-Aurora p-T288	rabbit	E. Pugacheva, Univ. of West Virginia, VA
anti-Wnt5a	goat	R&D Systems, Minneapolis, MN
anti-HEF1/NEDD9	mouse	Cell Signaling, Danvers, MA
Anti-Acetylated α-tubulin	mouse	Sigma, St. Louis, MO
Anti-Detyrosinated tubulin (Glu-tubulin)	rabbit	Chemicon, Billerica, MA
anti-α-tubulin	mouse	Sigma, St. Louis, MO
anti-Cyclin A	rabbit	SantaCruz, Santa Cruz, CA
FITC-conjugated anti-γ-tubulin	goat	SantaCruz, Santa Cruz, CA
anti-p-Erk1/2	mouse	Cell Signaling, Danvers, MA
anti-HA	mouse	Berkeley Antibody, Richmond, CA
anti-Flag	mouse	Sigma, St. Louis, MO
anti-Smad3	rabbit	Cell Signaling, Danvers, MA
anti-Smad2/3	mouse	SantaCruz, Santa Cruz, CA
anti-Axin1	rabbit	Cell Signaling, Danvers, MA